IWJ International Wound Journal

International Wound Journal ISSN 1742-4801

ORIGINAL ARTICLE

Interactions of manufactured silver nanoparticles of different sizes with normal human dermal fibroblasts

Alicia Avalos, Ana I Haza, Diego Mateo & Paloma Morales

Departamento de Nutrición, Bromatología y Tecnología de los Alimentos, Facultad de Veterinaria, Universidad Complutense de Madrid, Madrid, Spain

Key words
Cytotoxicity; Normal human dermal fibroblasts; Reactive oxygen species; Silver nanoparticles

Correspondence to
P Morales
Departamento de Nutrición, Bromatología y Tecnología de los Alimentos
Facultad de Veterinaria
Universidad Complutense de Madrid
28040 Madrid
Spain
E-mail: pmorales@vet.ucm.es

doi: 10.1111/iwj.12244

Avalos A, Haza AI, Mateo D, Morales P. Interactions of manufactured silver nanoparticles of different sizes with normal human dermal fibroblasts. Int Wound J 2016; 13:101–109

Abstract

Silver compounds have been used for their medicinal properties for centuries. At present, silver nanoparticles (AgNPs) are reemerging as a viable topical treatment option for infections encountered in burns, open wounds and chronic ulcers. This study evaluated the in vitro mechanisms of two different sizes of AgNPs (4·7 and 42 nm) toxicity in normal human dermal fibroblasts. The toxicity was evaluated by observing cell viability and oxidative stress parameters. In all toxicity endpoints studied (MTT and lactate dehydrogenase assays), AgNPs of 4·7 nm were much more toxic than the large AgNPs (42 nm). The cytotoxicity of both AgNPs was greatly decreased by pre-treatment with the antioxidant N-acetyl-L-cysteine. The oxidative stress parameters showed significant increase in reactive oxygen species levels, depletion of glutathione level and slight, but not statistically significant inactivation of superoxide dismutase, suggesting generation of oxidative stress. Thus, AgNPs should be used with caution for the topical treatment of burns and wounds, medical devices etc, because their toxicity depends on the size, the smaller NPs being much more cytotoxic than the large.

Introduction

The prefix 'nano' is derived from the Greek word 'nanos' meaning 'dwarf'. Nanotechnology involves the manipulation and application of engineered particles or systems that have at least one dimension less than 100 nanometres (nm) (1). On 18 October 2011, the European Commission defined 'nanomaterial' as 'a natural, incidental or manufactured material containing particles, in an unbound state or as an aggregate or as an agglomerate and where, for 50% or more of the particles in the number size distribution, one or more external dimensions is in the size range 1 nm–100 nm'. Application of this novel technology is now widely spread throughout all areas of life and still expanding. With the reduction in their size and concomitant increase in their specific surface area per unit mass, the nanoparticles (NPs) possess unique physico-chemical properties, which have led to these small objects becoming attractive and useful research and production units (2).

However, the same characteristic making NPs so attractive to be used in new products have led to concerns that NPs may pose a risk for humans and the environment (3). So, an improved understanding of the potential risks comprising exposure and hazard assessments, associated with exposure to nanomaterials is necessary (4) to check their toxicity or safety. Toxicological investigations of NPs imply that size, shape, chemical composition, surface charge, solubility, their ability to bind and affect biological sites as well as their metabolism and excretion influence the toxicity of NPs (5,6). For example, NPs of smaller size can enter the mitochondria of cells through various pathways, subsequently inducing oxidative stress and cell death via apoptosis (7). This is also reflected in a scientific opinion by the European Food Safety Authority (EFSA) Scientific Committee who concluded from the existing studies that NPs might

Key Messages

- silver nanoparticles (AgNPs) are used for the treatment of wounds and burns, and little is known about their toxicity
- in this study, the cytotoxic effect of AgNPs of different sizes (4·7 and 42 nm) on normal human dermal fibroblasts was evaluated
- the results showed a size-dependent toxicity. This toxicity may be due to oxidative stress, as the cellular antioxidant status was disturbed

Table 1 Characteristics of silver nanoparticles (AgNPs) obtained from Nanogap

Code	Particles	Average*± SD (nm)	Dispersion solution	Density (g/ml)	Density of particle (part/l)	Colour	pH
2106-W	AgNP 4·7	4·7 ± 1	Aqueous solution with PEI and PVP	1·024	$1{\cdot}75 \times 10^{19}$	Black, yellow (when diluted)	9·3
2103-W	AgNP 42	42 ± 9	Aqueous solution	1·01	Nd	Brown	Nd

Nd, no information provided; PEI, polyetherimide; PVP, polyvinylpyrrolidone.
*As provided by company.

have different toxicological properties than the bulk substance, but their risks should be assessed on a case-by-case basis (8).

It is estimated that of all the nanomaterials used in consumer products, silver nanoparticles (AgNPs) currently have the highest degree of commercialisation (9). Owing to their strong antibacterial property, AgNPs are largely used as a component of various commercially available products such as textiles, medical devices, contraceptives, water disinfectants and room spray (10–12). Moreover, AgNPs are used for the treatment of wounds and burns, as well as for coating on implants (13). Despite the increasing use of AgNPs in commercial products, little is known about the toxicity and cellular responses to AgNPs, and therefore the potential impacts of AgNPs on human and environmental health.

Because of the extensive presence of AgNPs in textiles, wound dressing, sport clothing and other products that come in direct contact with the skin, dermal exposure must be carefully evaluated. Some authors suggested an increased dermal penetration of AgNPs associated with damaged skin during in vitro experiments (14) or following the use of AgNPs-coated dressings in case of extensive burns (15). Keratinocytes in culture were used to assess the cytotoxic effects of AgNPs released from several types of silver-containing dressings, and the result of these studies showed that keratinocyte proliferation was significantly inhibited after exposure to extracts of nanocrystalline-coated dressings (16,17). The toxicity of AgNPs has also been investigated in others cell types, including BRL3A rat liver cells (18), PC-12 neuroendocrine cells (19), human alveolar epithelial cells (20) and germline stem cells (21). The toxicity of AgNPs is mainly due to oxidative stress (22). AgNPs were reported to act via reactive oxygen species (ROS) generation and glutathione depletion (18). The depletion of antioxidants including glutathione and protein-bound sulphydryl groups and the increase in activity of various antioxidant enzymes indicative of lipid peroxidation have been implicated in oxidative damage of cell molecules (23).

For in vitro studies with AgNPs, the selection of cell types representing the target tissue is very important. Assessment of human fibroblast cytotoxicity in vitro has been a useful tool for characterising cell toxicity of topically applied antiseptics (24). In this study, normal human dermal fibroblasts (NHDF) have been used because it is relevant to consider the implications of dermal exposure to AgNPs, due to exploitation of these NPs within wound dressings (25).

The main goal of the present work was to study how AgNPs of different sizes (4·7 and 42 nm) interact with normal human dermal fibroblast in order to understand the impact of such nanomaterials on cellular biological functions. In addition, total glutathione content, activity of superoxide dismutase (SOD) and ROS generation were used to evaluate feasible mechanisms by which AgNPs exerted their toxicity.

Material and methods

Chemicals

All chemicals were reagent-grade or higher and were obtained from Sigma–Aldrich (St Louis, MO), unless otherwise specified. Water-based solutions of AgNPs of 4·7 and 42 nm in diameter were purchased from Nanogap Subparticles (A Coruña, Spain). A summary of the characterisation according to the manufacturer's data is available in Table 1. Stock solutions of AgNPs were diluted to the required concentrations using the respective cell culture medium. N-acetyl-L-cysteine (NAC) was purchased from Sigma–Aldrich.

Characterisation of nanoparticles

The characterisation of AgNPs to determine their primary sizes and their morphology in aqueous solution by transmission electron microscopy (TEM) was conducted in previous studies (26). Dynamic light scattering (DLS) was used for characterisation of hydrodynamic size of AgNPs after incubation in cell-free culture media (0·02% v/v) for 24 hours at 37°C, performed on a Malvern Instruments Zetasizer Nano-ZS from Instituto Nacional de Investigación y Tecnología Agraria y Alimentaria (INIA), Madrid, Spain, as described by Murdock *et al.* (27). The method yields a hydrodynamic diameter, which is calculated particle diameter of a sphere that has the same measured motion in the solute as the actual particle.

Cell culture

NHDF were purchased from commercial PromoCell GmbH (Heidelberg, Germany). NHDF were cultured as monolayer in Fibroblast Basal medium supplemented with 2% v/v foetal calf serum, 1 ng/ml basic fibroblast growth factor and 5 µg/ml insulin. Culture medium and supplements were purchased from PromoCell GmbH. The human cell culture was incubated at 37°C and 100% humidity in a 5% CO_2 atmosphere.

Cytotoxicity endpoints

MTT [3-(4,5-dimethylthiazol-2-yl)-2,5-diphenyltetrazolium bromide] reduction and lactate dehydrogenase (LDH) leakage were used as parameters for cytotoxicity assessment. The MTT assay was assessed according to the manufacturer's

instructions (Cell Proliferation Kit I; Roche, Indianapolis, IN). Briefly, NHDF (5×10^5 cells/ml) were plated onto multiwell systems and incubated for 24 hours. After seeding, 100 µl of different concentrations of AgNPs (0·84–2000 µg/ml) or negative (without AgNPs) and positive controls [20 mM of N-nitrosodibutylamine, NDBA, 5% cell viability; (28)] were added to the wells and the plates were incubated for 24, 48 and 72 hours at 37°C and 100% humidity in a 5% CO_2 atmosphere. In order to reduce agglomeration, the AgNPs suspensions were mixed using vortex for 20 seconds and sonicated for 30 minutes. The optical density (OD) of each well was read at 620 nm (test wavelength) and 690 nm (reference wavelength) by an enzyme-linked immunosorbent assay (ELISA) with a built-in software package for data analysis (iEMS Reader MF, Labsystems; Helsinki, Finland).

The percentage of cell survival [% succinate dehydrogenase (SDH)] is defined as the ratio of the number of cells in the presence of AgNPs to the number in the absence of AgNPs; that is, $\%\text{SDH activity} = (A_1/A_0) \times 100$, where A_1 is the absorbance of the cells exposed to the AgNPs and A_0 is the absorbance of the negative control. All the concentrations were tested in 12 replicates and values presented in this article are mean ± standard deviation of three independent experiments.

Membrane integrity was assessed by measuring extracellular LDH according to the procedures described in manufacturer's instructions [Cytotoxicity Detection Kit (LDH)]. Briefly, NHDF were seeded in 96-well plates at a density of 5×10^5 cells/ml culture medium. After 24 hours of seeding, 100 µl of different concentrations of AgNPs (0·84–2000 µg/ml) or negative and positive controls were added to the wells and the plates were incubated for 24, 48 and 72 hours at 37°C and 100% humidity in a 5% CO_2 atmosphere. In order to reduce agglomeration previously, the AgNPs suspensions were mixed using vortex for 20 seconds and sonicated for 30 minutes. Cell-free culture media was collected from each well and incubated with a reaction mixture for 30 minutes. The plates were read with a microplate reader at 490 nm. A solution of 2% Triton X-100, which lead to 100% cytotoxicity through cell lysing and thus to maximum LDH leakage, was used as a positive control.

The release of LDH leakage was calculated as follows: LDH leakage (%) = (experimental value − untreated control)/(positive control − untreated control) × 100. All the concentrations were tested in 12 replicates and values presented in this article are mean ± standard deviation of three independent experiments.

Results obtained by the MTT and LDH assays were also expressed as EC_{50} values. The EC_{50} values represent the effective concentration of AgNPs that decreases the amount of viable cells to 50% of the maximum.

Protective effect of NAC against AgNPs-induced cytotoxicity

NAC is an important antioxidant and serves as a precursor for the synthesis of glutathione (29). The protective effect of NAC against AgNPs-induced cytotoxicity was evaluated using the MTT assay. Briefly, NHDF were pre-treated for 2 hours with NAC at different concentrations (1, 5, 10 and 20 mM) prior to a 24-hour treatment with the EC_{50} (concentration of AgNPs yielding 50% growth inhibition) of the corresponding AgNPs calculated by MTT assay. Then, the procedure is similar to the MTT assay described above.

Intracellular ROS measurement

ROS production was determined using 2′,7′-dichlorodihydrofluorescein diacetate (H_2DCFDA) from Molecules Probes (Eugene, OR). H_2DCFDA diffuses through the cell membrane and is hydrolysed by esterases to non-fluorescent dichlorofluorescein (DCFH). In the presence of ROS, this compound is oxidised to highly fluorescent dichlorofluorescein (DCF). For these experiments, NHDF were seeded in 24-well plates at a density of 2×10^5 cells/ml culture medium. After seeding, 1 ml of AgNPs of 4·7 (3·36 µg/ml) and 42 nm (100 µg/ml) or positive control (20 mM NDBA, 90% ROS production; (28)) were added to the wells and the plates were incubated for 48, 24, 3 hours, and 30 and 15 minutes. Previously, we performed the assay with different concentration of AgNPs of 4·7 and 42 nm to select the highest ROS production. However, with AgNPs significant ROS production could only be measured at the lower concentrations. Then, 2×10^5 cells were washed with phosphate buffered saline (PBS) loaded for 30 minutes with H_2DCFDA (10 µM) and incubated in a water bath (37°C). Cells were kept on ice and fluorescence intensity was read immediately with a FACS Calibur flow cytometer (Becton & Dickinson, Franklin Lakes, NJ) and the CellQuest software (Centro de Microscopía y Citometría, UCM, Madrid, Spain). For each experiment, 10^4 cells were analysed.

Total glutathione content

The total glutathione content was measured using a commercial colorimetric assay kit, OxiSelect Total Glutathione (GSSG/GSH; Cell Biolabs, Inc.; San Diego, CA). The assay was assessed according to the manufacturer's instructions. Briefly, NHDF were treated with 24 hours MTT EC_{50} of the corresponding AgNPs for 24, 48 and 72 hours. After treatment, cells were centrifuged and washed with cold 1× PBS. The pellet was resuspended with 200–500 µl ice-cold 0·5% metaphosphoric acid (MPA), the cells were again centrifuged at 1200 rpm for 5 minutes at 4°C and the supernatant was collected. Then, 25 µl 1× glutathione reductase and 25 µl 1× NADPH were added in 96-well plate and after that 100 µl of the samples were added. Finally, 50 µl 1× chromogen was added and mixed briefly. Immediately, the absorbance was recorded at 405 nm at 2 minutes intervals for 10 minutes.

The total glutathione content was determined by comparison with the predetermined glutathione standard curve. The results were expressed as percentage of total glutathione (GSSG/GSH) content.

SOD activity

SOD activity was measured using a commercial colorimetric assay kit, OxiSelect Superoxide Dismutase Activity (Cell Biolabs, Inc., San Diego, CA). Briefly, NHDF were treated with 24 hours MTT EC_{50} of the corresponding AgNPs for 24, 48 and 72 hours. After treatment, cells were washed with ice-cold PBS

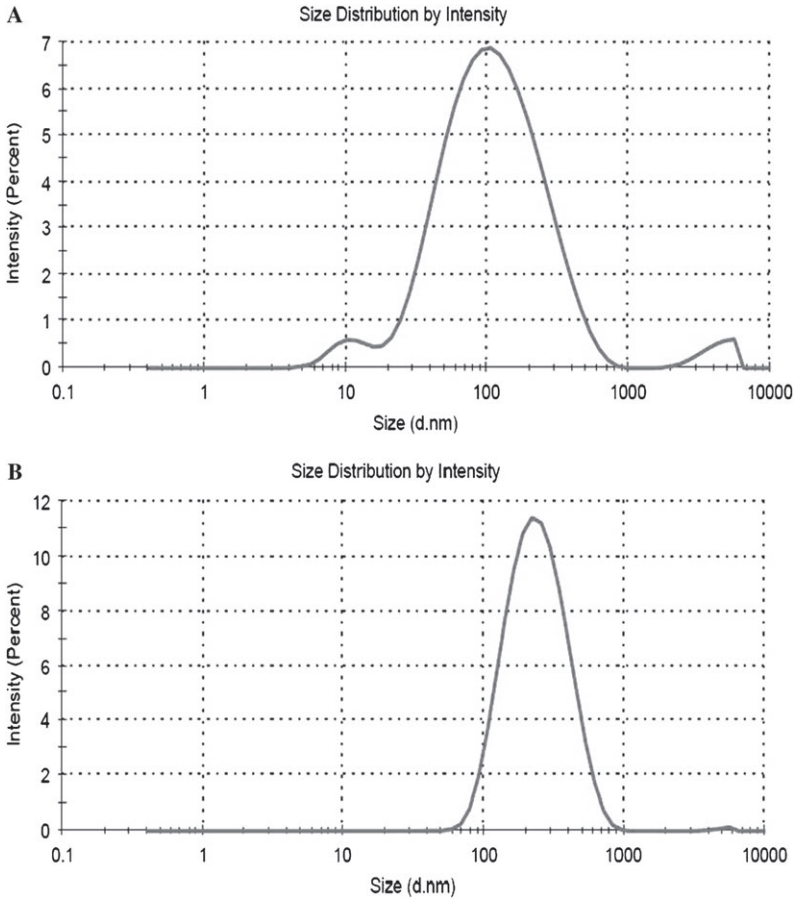

Figure 1 Dynamic light scattering (DLS) size distributions for 24 hours incubations of silver nanoparticles (AgNPs) 4·7 nm (panel A) and AgNPs 42 nm (panel B) in normal human dermal fibroblasts (NHDF) media.

and then were incubated on ice with 1× Lysis Buffer (10 mM Tris, pH 7·5, 150 mM NaCl, 0·1 mM EDTA, 0·5% Triton X-100) for 10 minutes. Later, cells were centrifuged at 12 000*g* for 10 minutes and the cell lysate supernatant was collected and added (10 µl) to 96-well plate and then the master mixture was added. Finally, 10 µl 1× Xanthine Oxidase Solution was added and immediately the absorbance was read at 490 nm.

The results were expressed as percentage of SOD activity and were calculated as follows: SOD activity $= [(A_0 - A_1)/A_0] \times 100$, where A_0 is the absorbance of the negative control and A_1 is the absorbance of the cells exposed to the AgNPs.

Statistical analyses

All means were calculated from three independent experiments and are expressed in the graphs as mean and standard deviation. The Student's *t*-test was used for statistical comparison and differences were considered significant at $P \leq 0{\cdot}05$. Descriptive and graphical methods were used to characterise the data. All tests were performed with the software package Statgraphics Plus 5·0 (Warrenton, VA).

Results

Characterisation of nanoparticles

The particle size, shape and size distribution of AgNPs of 4·7 and 42 nm in aqueous solution by TEM were conducted in previous studies in our laboratory (26). Results showed that majority of the AgNPs (both size) were approximately spherical, multifaceted or slightly elongated shape and well-dispersed. The size measurement of AgNPs of 4·7 and 42 nm showed a diameter of 5·5 nm ± 2·77 nm (SE) and 41·06 nm ± 9·29 nm, respectively. In this study, the particle size of the AgNPs of 4·7 and 42 nm in free culture media as imaged by DLS are shown in Figure 1. The DLS size analysis (Figure 1A) showed that AgNPs of 4·7 nm showed agglomeration in fibroblast media, with a major peak size at 138·9 nm (∼94% intensity) and two minor peaks at 10·84 and 4222 nm (∼3·3% and 2·7% intensity, respectively). AgNPs of 42 nm also showed agglomeration in fibroblast media, with peak size at 259·9 nm (∼99·7% intensity; Figure 1B).

Effect of AgNPs on cellular viability

MTT and LDH leakage, two cytotoxicity markers, were used to evaluate the effects of AgNPs on cellular viability. The results of the MTT assay showed a significant decrease of NHDF cell growth when exposed to AgNPs of 4·7 nm at the concentrations of 6·72 (13%, 8% and 9% of cell survival) and 13·45 µg/ml (12%, 8% and 6% of cell survival) for all treatment times. The EC_{50} value was 4·17 µg/ml ± 0·64 µg/ml at 24 hours of incubation (Figure 2). In parallel, results obtained by LDH assay showed that the percentage of LDH leakage presented a strong increase at concentrations of 6·72 (93%, 91% and 94% of LDH leakage) and 13·45 µg/ml (96%, 99% and 98% of LDH

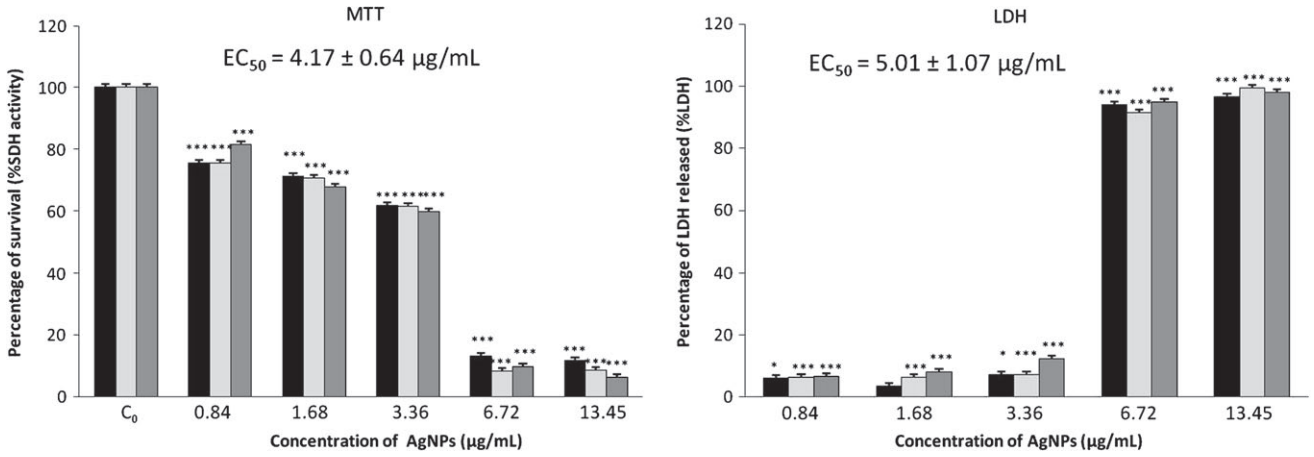

Figure 2 Effects of silver nanoparticles (AgNPs) 4·7 nm on normal human dermal fibroblasts (NHDF) cell viability by MTT and lactate dehydrogenase (LDH) assays. Cells were cultured with different doses of AgNPs for 24 (■), 48 (□) and 72 (▩) hours. C_0 – untreated cells. Asterisks indicate significant difference from control $***P \leq 0{\cdot}001$ and $*P \leq 0{\cdot}05$.

leakage), 5·01 µg/ml ± 1·07 µg/ml being the EC_{50} value after 24 hours of treatment.

Figure 3 shows the cytotoxic effect of AgNPs of 42 nm on NHDF cells. Data obtained by MTT assay showed a 50% reduction on cell viability after treatment with 2000 µg/ml AgNPs for all incubation times. These results were confirmed by LDH assay. The concentration of 2000 µg/ml AgNPs increased 52% of the LDH released, with EC_{50} value of 1959 µg/ml ± 7·39 µg/ml.

Protective effect of NAC against AgNPs-induced cytotoxicity

Among the multiple mechanisms that are attributed to NAC, highlights its antioxidant activity and therefore its ability to trap or react with ROS (30). AgNP-induced inhibition of MTT reduction was largely prevented by NAC (Figure 4). The viability of NHDF cells pre-treated with 20 mM NAC prior to a 24-hour treatment with 24 hours MTT EC_{50} of AgNPs of 4·7 nm increased to 100%. However, with the treatment of 24 hours MTT EC_{50} of AgNPs of 42 nm, cell viability increased to approximately 77% (5, 10 and 20 mM NAC). Thus, our results suggest that oxidative stress is primarily responsible for the cytotoxicity of AgNPs.

AgNP-derived induction of ROS

The generation of ROS and oxidative stress appear to be the two main mechanisms of toxicity (31). To investigate the potential role of oxidative stress induced by AgNPs, ROS generation was measured. After treatment of NHDF with AgNPs of 4·7 and 42 nm, DCF fluorescence was measured by flow cytometry and expressed as percentage of control. A significant increase of ROS levels was observed after treatment with AgNPs of 4·7 (3·36 µg/ml) and 42 nm (100 µg/ml), reaching the maximum signal after 3 and 24 hours treatment, respectively. ROS levels increased 2·41-fold (AgNPs of 4·7 nm) and 1·76-fold (AgNPs of 42 nm) more than the control (Figure 5).

Cellular antioxidant response

The action of intracellular molecular antioxidants (glutathione) and regulation of antioxidant enzymes activity, such as SOD are shown in Figures 6 and 7. Our data demonstrated that a significant depletion ($P < 0{\cdot}01$) of total glutathione content (GSSG/GSH) occurred in AgNPs (4·7 and 42 nm)-exposed cells. Total glutathione content (GSSG/GSH) in NHDF exposed to 24 hours MTT EC_{50} of AgNPs of 4·7 nm, reduced approximately to 5% relative to control, for 24, 48 and 72 hours (Figure 6). The treatment with 24 hours MTT EC_{50} of AgNPs of 42 nm depleted GSSG/GSH to 29·5% (24 hours) and 3·7% (48 and 72 hours) relative to the controls (Figure 6).

The activity of antioxidant enzymes was also modulated (Figure 7). SOD activity was very slightly reduced after NHDF treatment with the 24 hours MTT EC_{50} of AgNPs of 4·7 and 42 nm for 24, 48 and 72 hours (approximately 8% and 17% relative to controls, respectively), but this reduction was not statistically significant.

Discussion

AgNPs have been integrated into hundreds of products that affect the daily lives of millions of people in many countries. According to the silver nanotechnology commercial inventory (SNCI) (32), only 45% of the listed products reported the NP size used in the product, ranging from 0·3 nm to 250 nm, 24 nm being the average NP size of all reported products. Their main use is for disinfection in wound care and in products such as odour-reducing clothing, acne creams and face masks. However, despite their widespread use, information on how companies synthesised the AgNPs and the characteristics of these or how they specifically integrated it into their product is lacking. Most of these products come into direct contact with skin, the largest organ of the human body, and could serve as a potential route for NP penetration. Therefore, the relationship of AgNPs in skin needs to be investigated. In the wound healing process, dermal fibroblasts are the main cell types implicated in the extracellular matrix production (33). Considering this fact,

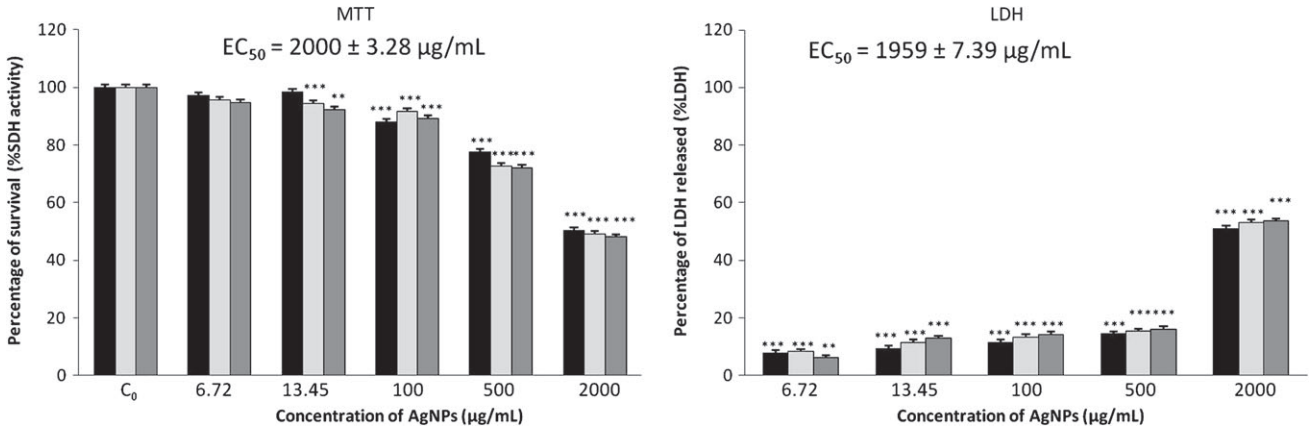

Figure 3 Effects of silver nanoparticles (AgNPs) 42 nm on normal human dermal fibroblasts (NHDF) cell viability by MTT and lactate dehydrogenase (LDH) assays. Cells were cultured with different doses of AgNPs for 24 (■), 48 (□) and 72 (▩) hours. C_0 – untreated cells. Asterisks indicate significant difference from control $***P \leq 0{\cdot}001$ and $**P \leq 0{\cdot}01$.

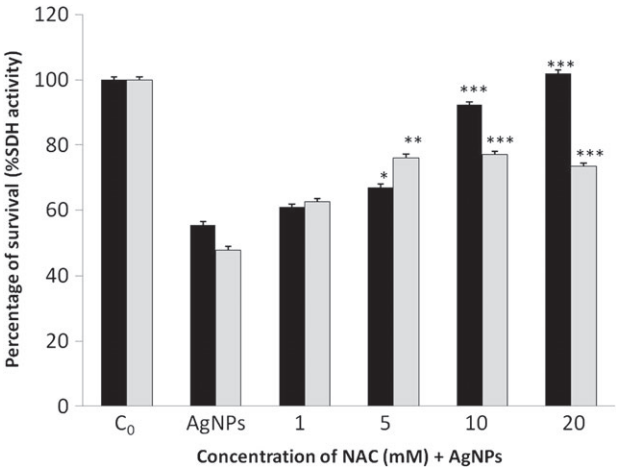

Figure 4 Protective effects of N-acetyl-L-cysteine (NAC) against treatment with 24 hours MTT EC_{50} doses of silver nanoparticles (AgNPs) of 4·7 (■) and 42 nm (□) in normal human dermal fibroblasts (NHDF) cell viability by MTT assay. Cells were cultured with different doses of NAC for 24 hours. Asterisks indicate significant difference from control $***P \leq 0{\cdot}001$, $**P \leq 0{\cdot}01$ and $*P \leq 0{\cdot}05$.

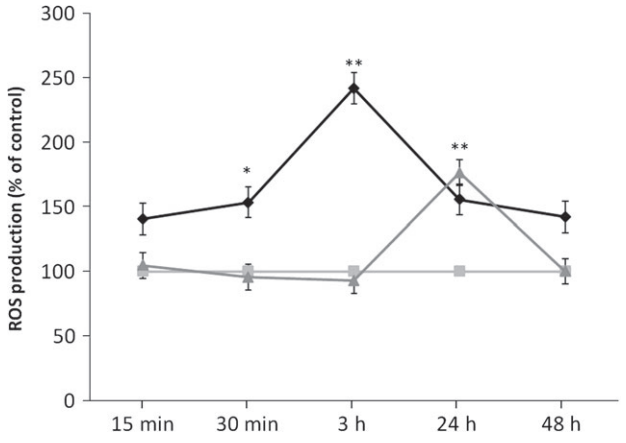

Figure 5 Time-course of reactive oxygen species (ROS) production in untreated normal human dermal fibroblasts (NHDF) cells (□) and treated with silver nanoparticles (AgNPs) of 4·7 nm (◆) or AgNPs of 42 nm (▲). Asterisks indicate significant difference from control $**P \leq 0{\cdot}01$ and $*P \leq 0{\cdot}05$.

in this study we have selected NHDF cell line to evaluate the cytotoxic potential of AgNPs of various sizes.

The physico-chemical characteristics of NPs play a significant role in their effect on biological systems (34,35). The principal parameters of NPs are their shape, size, surface area and the morphological substructure of the substance. Other very important parameter is the state of agglomeration. Agglomeration is known to occur with the majority of engineered NPs with high surface activity (36). In addition, agglomeration of NPs has been demonstrated to have a profound impact on their toxicity in vitro (37). In this study, AgNPs were found to agglomerate within NHDF culture media (Figure 1). After incubation on NHDF media, the diameter of AgNP 4·7 nm increased to138·9 nm, which was around 29 times larger than the primary particle sizes obtained using DLS technique. The diameter of AgNP 42 nm also increased to 259·9 nm after incubation on NHDF media, around six times larger than the primary particle sizes. These results indicate the possible interaction of AgNPs with the cell culture media, which have been widely reported with different NPs that leads to the formation of 'protein corona' (38,39). Therefore, not only the size of the primary NPs but also the size of the secondary NPs could be used as a characteristic parameter to determine the in vitro toxicity of NPs in a cell culture medium (40).

Viability assays are vital steps in toxicology that explain the cellular response to a toxicant. Also, they give information on cell death, survival and metabolic activities. The use of several viability assays is important to determine the optimal assay to assess AgNPs toxicity; therefore, mortality of NHDF cells after AgNPs exposure was evaluated with two different assays, MTT and LDH, which use colorimetric markers to determine cell viability by assessing cell metabolism. The two assays showed that both AgNPs (4·7 and 42 nm) contributed to a decrease in NHDF viability. Arora *et al.* (41)

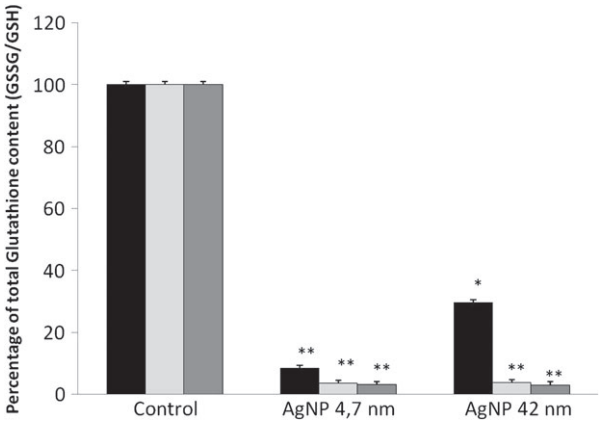

Figure 6 Effects of silver nanoparticles (AgNPs) of 4·7 and 42 nm in the total glutathione content on normal human dermal fibroblasts (NHDF) cells. Cells were cultured with 24 hours MTT EC_{50} doses of AgNPs for 24 (■), 48 (□) and 72 (▩) hours. Control – untreated cells. Asterisks indicate significant difference from control $**P \leq 0{\cdot}01$ and $*P \leq 0{\cdot}05$.

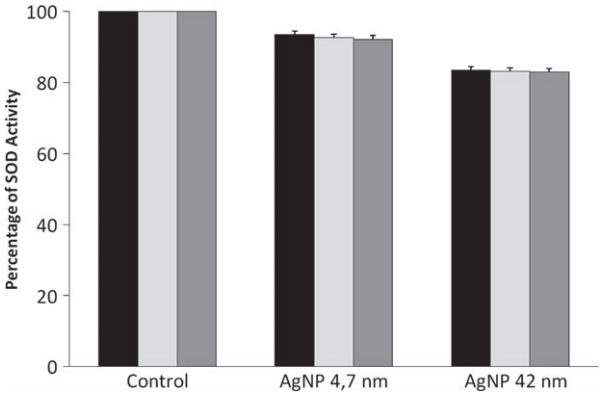

Figure 7 Effects of silver nanoparticles (AgNPs) of 4·7 and 42 nm in the superoxide dismutase (SOD) activity on normal human dermal fibroblasts (NHDF) cells. Cells were cultured with 24 hours MTT EC_{50} doses of AgNPs for 24 (■), 48 (□) and 72 (▩) hours.

also observed a decrease in dermal fibroblasts viability after treatment with AgNPs of 7–20 nm. Furthermore, the AgNPs have also shown to be cytotoxic to mouse fibroblasts (L929), human fibrosarcoma (HT-1080) and normal human lung fibroblasts (IMR-90) (42–44). Viability reduction based upon the EC_{50} values was size-dependent and AgNPs of 4·7 and 42 nm exhibited a dramatic difference in cytotoxicity. Small AgNPs (4·7 nm) were much more cytotoxic than large NPs (42 nm). The AgNPs of 4·7 nm exhibited an EC_{50} value of 4·17 μg/ml and 5·01 μg/ml (MTT and LDH, respectively),whereas the EC_{50} AgNPs of 42 nm was 2000 μg/ml and 1959 μg/ml (MTT and LDH, respectively), about 400-fold less cytotoxic. According to this fact, particle size has been demonstrated to influence toxicity (31,42,45,46), tissue distribution (47), intestine and dermal penetration (48) and cellular uptake (49). In general, greater effects were observed for smaller NPs. Accordingly, smaller NPs have a wider tissue distribution, penetrate further within the skin and intestine, are internalised to a greater extent and have a larger toxic potency (25).

It has been suggested that the general trend of NP cytotoxicity is similar among various types of NPs (50) and that non-specific oxidative stress is one of the largest concerns in NP-induced toxicity (51,29,52). Consistent with those findings, our results showed that the cytotoxicity induced by AgNPs (4·7 and 42 nm) was efficiently prevented by NAC treatment (Figure 4). These findings suggest that oxidative stress is primarily responsible for the cytotoxicity of AgNPs. A number of studies have implicated the production of ROS in cytotoxicity mediated by NPs (53). In our study, a fluorogenic assay was used to measure the production of ROS at different times. The results showed that there was a significant increase in ROS after treatment with AgNPs. AgNPs of 4·7 nm induced drastic increase in ROS production on NHDF cells after 3 hours (241%). However, AgNPs of 42 nm induced a lower ROS production (176%) on NHDF cell line after 24 hours than AgNPs of 4·7 nm. Thus, ROS production on NHDF was also dependent on the particle size. Carlson *et al.* (54) observed similar results in macrophages, as smaller AgNPs (15 nm) showed the highest production ROS. It is recognised that there is a direct relationship between surface area and ROS generation capability. Smaller NPs possessed greater surface area per unit mass, leading to a larger number of atoms or molecules to be displayed on the surface instead of the interior of the particles. Therefore, lots of active sites were created on the particle surface, which could capture oxygen molecules and produce superoxide radicals as well as other kinds of ROS through dismutation (29).

To confirm the possible role of oxidative stress as a mechanism of AgNPs-induced toxicity, the effects on total glutathione content and SOD activity were monitored. GSH is an important antioxidant and ROS scavenger of the cell. Thus, preserving the GSH-mediated antioxidant defence is critical for cell survival (55–57). In our study, the total gluthatione content was completely depleted in NHDF exposed to AgNPs of 4·7 and 42 nm after 72 hours (95–96%). Other authors such as Arora *et al.* (43), Carlson *et al.* (54) and Piao *et al.* (58), also observed decreased levels of GSH after treatment with AgNPs. However, the changes observed in the activity of SOD were not statistically significant in NHD after treatment with AgNPs of 4·7 and 42 nm. This result is suggestive of a differential and less pronounced response by these cellular defence mechanisms as compared with GSH. Arora *et al.* (41) did not observed statistically significant changes in the levels of SOD on fibroblast after treatment with AgNPs.

Conclusions

Size measurement study of AgNPs in the cell culture media showed the interaction of AgNPs with the NHDF media components that suggest significant protein adsorption by the NPs in the cell growth media. Small AgNPs (4·7 nm) were found to be much more cytotoxic than large AgNPs (42 nm). In addition, the cytotoxicity induced by AgNPs was efficiently prevented by NAC treatment. This fact together with the increased generation of ROS and decreased levels of total gluthatione content observed, support the hypothesis that the cells are undergoing oxidative stress, which could ultimately lead to the observed cytotoxicity. Thus, AgNPs should be used with caution for the topical treatment of burns, wounds, medical devices etc.,

because their toxicity depends on the size, the smaller NPs being much more cytotoxic than the large. Abnormal elevation of blood silver level and argyria-like symptoms following the use of AgNPs (15 nm)-coated dressings for burns were described in one clinical report (15). Elevated liver enzyme levels were also evident, insinuating that liver injury had occurred as a consequence of treatment. Hence, this case study provided evidence that silver is able to become systematically available following dermal contact.

Acknowledgements

This work has been supported by grant AGL2010-16561 from the Ministerio de Educación, Cultura y Deporte (Spain). AA is a recipient of a fellowship from the Ministerio de Educación, Cultura y Deporte (Spain). We thank the Instituto Nacional de Investigación y Tecnología Agraria y Alimentaria (INIA), Madrid, Spain for the use of DLS equipment.

References

1. Hoyt VW, Mason E. Nanotechnology: emerging health issues. *J Chem Health Saf* 2008;**15**:10–5.
2. Chairuangkitti P, Lawanprasert S, Roytrakul S, Aueviriyavit S, Phummiratch D, Kulthong K, Chanvorachote P, Maniratanachote R. Silver nanoparticles induce toxicity in A549 cells via ROS-dependent and ROS-independent pathways. *Toxicol In Vitro* 2013;**27**:330–8.
3. Beer C, Foldbjerg R, Hayashi Y, Sutherland DS, Autrup H. Toxicity of silver nanoparticles - nanoparticle or silver ion? *Toxicol Lett* 2012;**208**:286–92.
4. Maynard AD, Aitken RJ, Butz T, Colvin V, Donaldson K, Oberdorster G, Philbert MA, Ryan J, Seaton A, Stone V, Tinkle SS, Walker NJ, Warheit DB. Safe handling in nanotechnology. *Nature* 2006;**444**:267–9.
5. Castranova V. Overview of current toxicological knowledge of engineered nanoparticles. *J Occup Environ Med* 2011;**53**:14–7.
6. Schrand AM, Rahman MF, Hussain SM, Schlager JJ, Smith DA, Syed AF. Metal-based nanoparticles and their toxicity assessment. *Wiley Interdiscip Rev Nanomed Nanobiotechnol* 2010;**2**:544–68.
7. Xia T, Kovochich M, Nel AE. Impairment of mitochondrial function by particle matter (PM) and their toxic components: implications for PM-induced cardiovascular and lung disease. *Front Biosci* 2007;**12**:1238–46.
8. EFSA Scientific Committee. Guidance on the risk assessment of the application of nanoscience and nanotechnologies in the food and feed chain. *EFSA Journal* 2011;**9**:2140.
9. Henig RM. Our silver-coated future. *OnEarth* 2007;23–9.
10. Vigneshwaran N, Kathe AA, Varadarajan PV, Nachane RP, Balasubramanya RHJ. Functional finishing of cotton fabrics using silver nanoparticles. *J Nanosci Nanotechnol* 2007;**7**:1893–7.
11. Samuel U, Guggenbichler JP. Prevention of catheter-related infections: the potential of a new nano-silver impregnated catheter. *Int J Antimicrob Agents* 2004;**23**:75–8.
12. Gosheger G, Hardes J, Ahrens H, Streitburger A, Buerger H, Erren M, Gunsel A, Kemper FH, Winkelmann W, Von EC. Silver-coated megaendoprostheses in a rabbit model-an analysis of the infection rate and toxicological side effects. *Biomaterials* 2004;**25**: 5547–56.
13. Margaret IP, Sau LL, Vincent KMP, Ivan L, Andrew B. Antimicrobial activities of silver dressings: an in vitro comparison. *J Med Microbiol* 2006;**55**:59–63.
14. Larese FF, D'Agostin F, Crosera M, Adami G, Renzi N, Bovenzi M, Maina G. Human skin penetration of silver nanoparticles through intact and damaged skin. *Toxicology* 2009;**255**:33–7.
15. Trop M, Novak M, Rodl S, Hellbom B, Kroell W, Goessler W. Silver coated dressing acticoat caused raised liver enzymes and argyria-like symptoms in burn patient. *J Trauma* 2006;**60**:648–52.
16. Paddle-Ledinek JE, Nasa Z, Cleland HJ. Effect of different wound dressings on cell viability and proliferation. *Plast Reconstr Surg* 2006;**117**:110–8.
17. Lam PK, Chan ES, Ho WS, Liew CT. In vitro cytotoxicity testing of a nanocrystalline silver dressing (acticoat) on cultured keratinocytes. *Br J Biomed Sci* 2004;**61**:125–7.
18. Hussain SM, Hess KL, Gearhart JM, Geiss KT, Schlager JJ. In vitro toxicity of nanoparticles in BRL 3A rat liver cells. *Toxicol In Vitro* 2005;**19**:975–83.
19. Hussain S, Javorina A, Schrand A, Duhart H, Ali S, Schlager J. The interaction of manganese nanoparticles with PC-12 cells induces dopamine depletion. *Toxicol Sci* 2006;**92**(Suppl 2):456–63.
20. Park S, Lee YK, Jung M, Kim KH, Chung N, Ahn EK, Lim Y, Lee KH. Cellular toxicity of various inhalable metal nanoparticles on human alveolar epithelial cells. *Inhal Toxicol* 2007;**19**(Suppl 1):59–65.
21. Braydich-Stolle L, Hussain S, Schlager JJ, Hofmann MC. In vitro cytotoxicity of nanoparticles in mammalian stem cells. *Toxicol Sci* 2005;**88**:412–9.
22. Kim S, Choi JE, Choi J, Chung K, Park K, Yi J, Ryu D. Oxidative stress-dependent toxicity of silver nanoparticles in human hepatoma cells. *Toxicol In Vitro* 2009;**23**:1076–84.
23. Ahamed M, Siddiqui MKJ. Low level lead exposure and oxidative stress: current opinions. *Clin Chim Acta* 2007;**383**:57–64.
24. Hidalgo E, Bartolome R, Barroso C, Moreno A, Dominguez C. Silver nitrate: antimicrobial activity related to cytotoxicity in cultured human fibroblasts. *Skin Pharmacol Appl Skin Physiol* 1998;**11**:140–51.
25. Johnston HJ, Hutchison G, Christensen FM, Peters S, Hankin S, Stone V. A review of the in vivo and in vitro toxicity of silver and gold particulates: particle attributes and biological mechanisms responsible for the observed toxicity. *Crit Rev Toxicol* 2010;**40**:328–46.
26. Ávalos A, Haza AI, Mateo D, Morales P. Cytotoxicity and ROS production of manufactured silver nanoparticles of different sizes in hepatoma and leukemia cells. *J Appl Toxicol* 2013. DOI: 10.1002/jat.2957.
27. Murdock RC, Braydich-Stolle L, Schrand AM, Schlager JJ, Hussain SM. Characterization of nanomaterial dispersion in solution prior to in vitro exposure using dynamic light scattering technique. *Toxicol Sci* 2008;**101**:239–53.
28. García A, Morales P, Arranz N, Delgado E, Rafter J, Haza AI. Induction of apoptosis and reactive oxygen species production by *N*-nitrosopiperidine and *N*-nitrosodibutylamine in human leukemia cells. *J Appl Toxicol* 2008;**28**:455–65.
29. Nel A, Xia T, Mädler L, Li N. Toxic potential of materials at the nanolevel. *Science* 2006;**311**:622–7.
30. Zafarullah M, Li WQ, Sylvester J, Ahmad M. Molecular mechanisms of N-acetylcysteine actions. *Cell Mol Life Sci* 2003;**60**:6–20.
31. Hsin YH, Chen CF, Huang S, Shih TS, Lai PS, Chueh PJ. The apoptotic effect of nanosilver is mediated by ROS- and JNK dependent mechanism involving the mitochondrial pathway in NIH3T3 cells. *Toxicol Lett* 2008;**179**:130–9.
32. Fauss E. *The silver nanotechnology commercial inventory*. Virginia Univ, 2008.
33. Hunt TK, Hopt HW. Wound healing and infection, what surgeons and anesthesiologist can do? *Surg Clin North Am* 1997;**77**:587–606.
34. Oberdörster G, Finkelstein JN, Johnston C, Gelein R, Cox C, Baggs R, Elder ACP. Acute pulmonary effects of ultrafine particles in rats and mice. *Res Rep Health Eff Inst* 2000;**96**:5–74.
35. Donaldson K, Stone V, Tran CL, Kreyling W, Borm PJA. Nanotoxicology. *Occup Environ Med* 2004;**61**:727–8.
36. Skebo JE, Grabinski CM, Schrand AM, Schlager JJ, Hussain SM. Assessment of metal nanoparticle agglomeration, uptake, and interaction using high-illuminating system. *Int J Toxicol* 2007;**26**:135–41.
37. Liu S, Wei L, Hao L, Fang N, Chang MW, Xu R, Yang Y, Chen Y. Sharper and faster ''nano darts'' kill more bacteria: a study of antibacterial activity of individually dispersed pristine single-walled carbon nanotube. *ACS Nano* 2009;**3**:3891–902.

38. Lynch I, Dawson K. Protein-nanoparticle interactions. *Nanotoday* 2008;**3**:40–7.
39. Lundqvist M, Stigler J, Elia G, Lynch I, Cerdevall T, Dawson K. Nanoparticle size and surface properties determine the protein corona with possible implications for biological impacts. *Proc Natl Acad Sci U S A* 2008;**105**:14265–70.
40. Kato H. In vitro assays: tracking nanoparticles inside cells. *Nat Nanotechnol* 2011;**6**:139–40.
41. Arora S, Jain J, Rajwade JM, Paknikar KM. Interactions of silver nanoparticles with primary mouse fibroblasts and liver cells. *Toxicol Appl Pharmacol* 2009;**236**:310–8.
42. Park MV, Neigh AM, Vermeulen JP, Fonteyne LJJ, Verharen HW, Briedé JJ, Loveren HV, Jong WH. The effect of particle size on the cytotoxicity, inflammation, developmental toxicity and genotoxicity of silver nanoparticles. *Biomaterials* 2011;**32**:9810–7.
43. Arora S, Jain J, Rajwade JM, Paknikar KM. Cellular responses induced by silver nanoparticles: in vitro studies. *Toxicol Lett* 2008;**179**:93–100.
44. Asharani PV, Grace LKM, Manoor PH, Suresh V. Cytotoxicity and genotoxicity of silver nanoparticles in human cells. *ACS Nano* 2009;**3**:279–90.
45. Cha K, Hong HW, Choi YG, Lee MJ, Park JH, Chae HK, Ryu G, Myung H. Comparison of acute responses of mice livers to short-term exposure to nano-sized or micro-sized silver particles. *Biotechnol Lett* 2008;**30**:1893–9.
46. Powers CM, Badireddy AR, Ryde IT, Seidler FJ, Slotkin TA. Silver nanoparticles compromise neurodevelopment in PC12 cells: critical contributions of silver ion, particle size, coating, and composition. *Environ Health Perspect* 2011;**119**:37–44.
47. De Jong WH, Hagens WI, Krystek P, Burger MC, Sips AJAM, Geertsma RE. Particle size-dependent organ distribution of gold nanoparticles after intravenous administration. *Biomaterials* 2008;**29**:1912–9.
48. Sonavane G, Tomoda K, Sano A, Ohshima H, Terada H, Makino K. In vitro permeation of gold nanoparticles through rat skin and rat intestine: effect of particle size. *Colloids Surf B Biointerfaces* 2008;**65**:1–10.
49. Chithrani BD, Ghazani AA, Chan WCW. Determining the size and shape dependence of gold nanoparticle uptake by mammalian cells. *Nano Lett* 2006;**6**:662–8.
50. Jin CY, Zhu BS, Wang XF, Lu QH. Cytotoxicity of titanium dioxide nanoparticles in mouse fibroblast cells. *Chem Res Toxicol* 2008;**21**:1871–7.
51. Colvin VL. The potential environmental impact of engineered nanomaterials. *Nat Biotechnol* 2003;**21**:1166–70.
52. Xia T, Kovochich M, Brant J, Hotze M, Sempf J, Oberley T, Sioutas C, Yeh JI, Wiesner MR, Nel AE. Comparison of the abilities of ambient and manufactured nanoparticles to induce cellular toxicity according to an oxidative stress paradigm. *Nano Lett* 2006;**6**:1794–807.
53. Foldbjerg R, Olesen P, Hougaard M, Dang DA, Hoffmann HJ, Autrup H. PVP-coated silver nanoparticles and silver ions induce reactive oxygen species, apoptosis and necrosis in THP-1 monocytes. *Toxicol Lett* 2009;**190**:156–62.
54. Carlson C, Hussain SM, Schrand AM, Braydich-Stolle LK, Hess KL, Jones RL, Schlager JJ. Unique cellular interaction of silver nanoparticles: size dependent generation of reactive oxygen species. *J Phys Chem B* 2008;**112**:13608–19.
55. Anderson MF, Nilsson M, Eriksson PS, Sims NR. Glutathione monoethyl ester provides neuroprotection in a rat model of stroke. *Neurosci Lett* 2004;**354**:163–5.
56. Dewarijee S, Maiti A, Sahu R, Dua TK, Mandal V. Effective control of type 2 diabetes through antioxidant defense by edible fruits of *Diospyros peregrina*. *Evid Based Complement Alternat Med* 2011;**2009**:1–7.
57. Sies H. Glutathione and its role in cellular functions. *Free Radic Biol Med* 1999;**27**:916–21.
58. Piao MJ, Kang KA, Lee IK, Kim HS, Kim S, Choi JY, Choi J, Hyun JW. Silver nanoparticles induce oxidative cell damage in human liver cells through inhibition of reduced glutathione and induction of mitochondria-involved apoptosis. *Toxicol Lett* 2011;**201**:92–100.